Supporting information for:

Interactions between a responsive microgel monolayer and a rigid colloid: from soft to hard interfaces

Steffen Bochenek,[†] Cathy E. McNamee,[‡] Michael Kappl,[¶] Hans-Juergen Butt,[¶] and Walter Richtering[†,§]

[†]*Institute of Physical Chemistry, RWTH Aachen University, Landoltweg 2, 52056 Aachen, Germany*

[‡]*Department of Chemistry and Materials, Faculty of Textile Science and Technology, Shinshu University, Tokida 3-15-1, Ueda, Nagano, 386-8567, Japan*

[¶]*Max Planck Institute of Polymer Research, Ackermannweg 10, 55128, Mainz, Germany*

[§]*JARA-SOFT, 52056 Aachen, Germany*

E-mail:

Characterization in Bulk
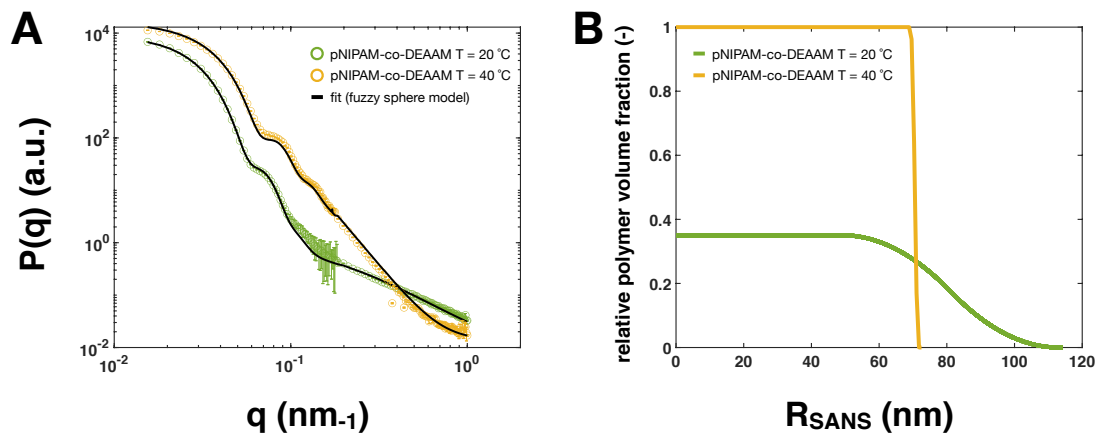
Figure S1: Small-angle neutron scattering data and fits of pNIPAM-co-DEAAM microgels. (A) Particle form factor, $P(q)$, *versus* scattering vector, q, with fits at T = 20° C and T = 40° C. (B) Relative polymer Volume fraction *versus* radius, R, from the fits of the fuzzy-sphere model in (A).
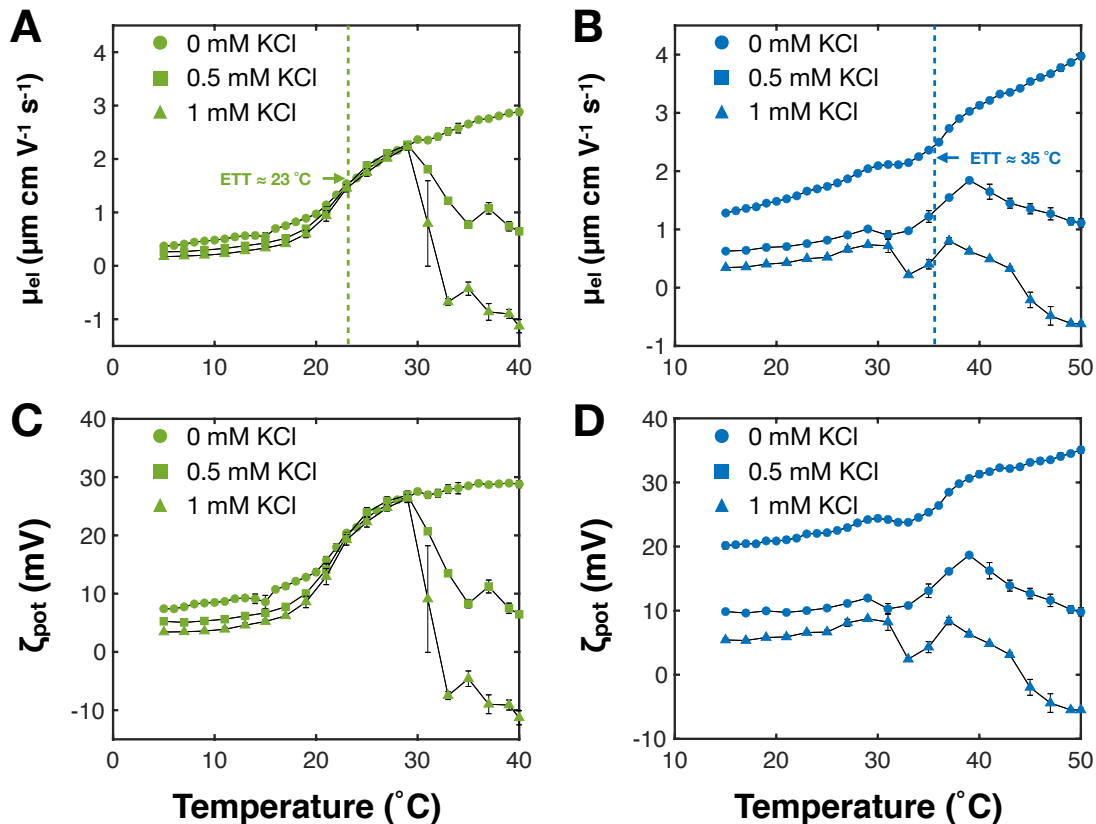
Figure S2: (A, B) Electrophoretic mobility and (C, D) zeta potential as a function of temperature for (A, C) pNIPAM-co-DEAAM and (B, D) pNIPAM microgels at different KCl concentrations. The dashed lines show the ETT of the microgels.
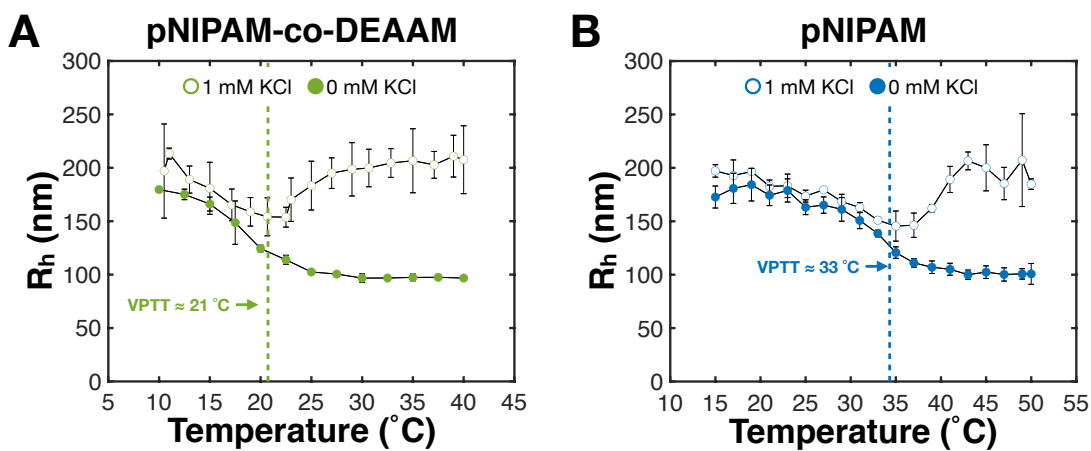
Figure S3: Temperature-dependent swelling of the microgels measured with dynamic light scattering in 0 and 1 mM KCl solution. Measurements were conducted with a NanoZS Zetasizer at a scattering angle of 173°. (A) pNIPAM-co-DEAAM microgels and (B) pNIPAM.

Force Distance Curves
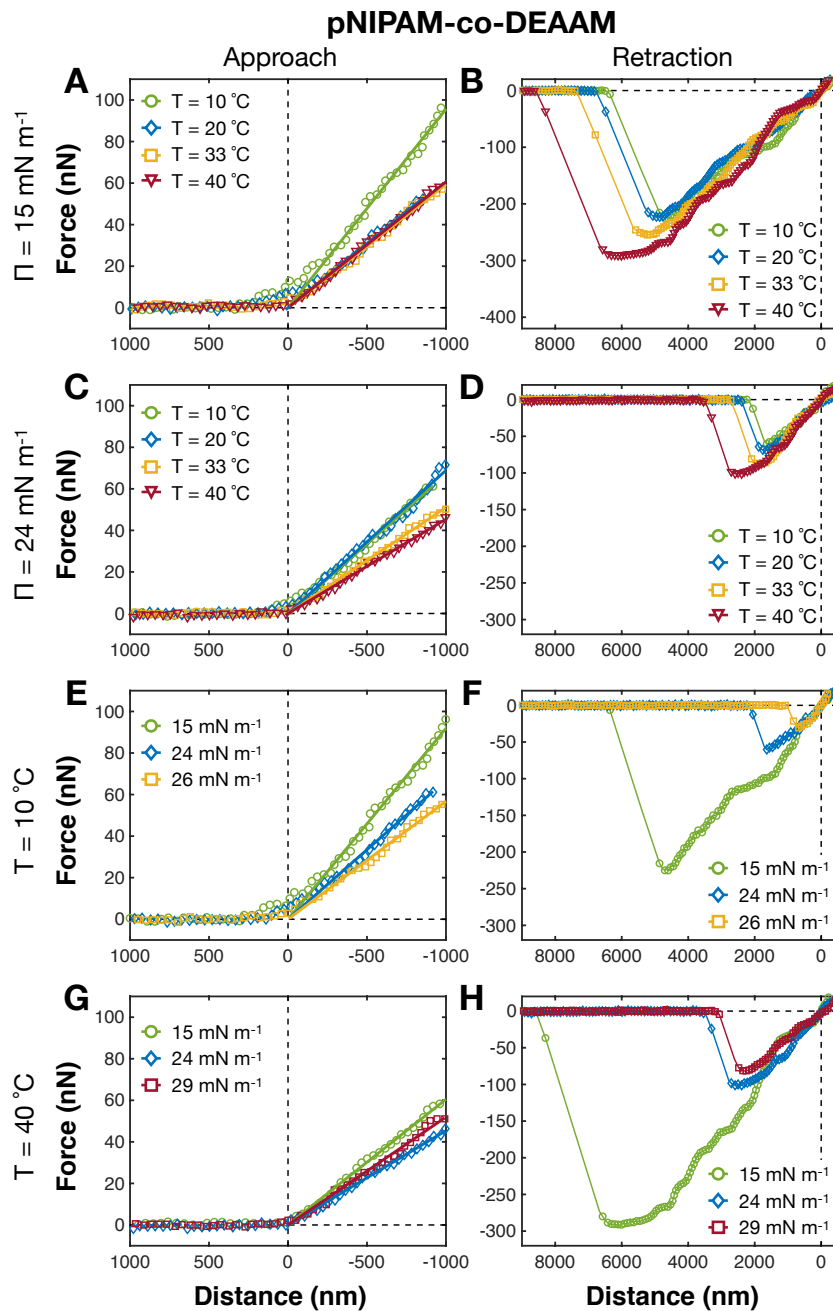
Figure S4: Examples of force-distance curves of pNIPAM-co-DEAAM microgel monolayers at the air-water interface measured with hydrophilpos probe from the aqueous phase. The probe has diameter of 6.84 μm. Approach (left) and retraction (right) force-distance curves. (A,B) F-D curves as a function of temperature. (C,D) F-D curves as a function of compression for T = 20 °C. (E,F) F-D curves as a function of compression for T = 40 °C.
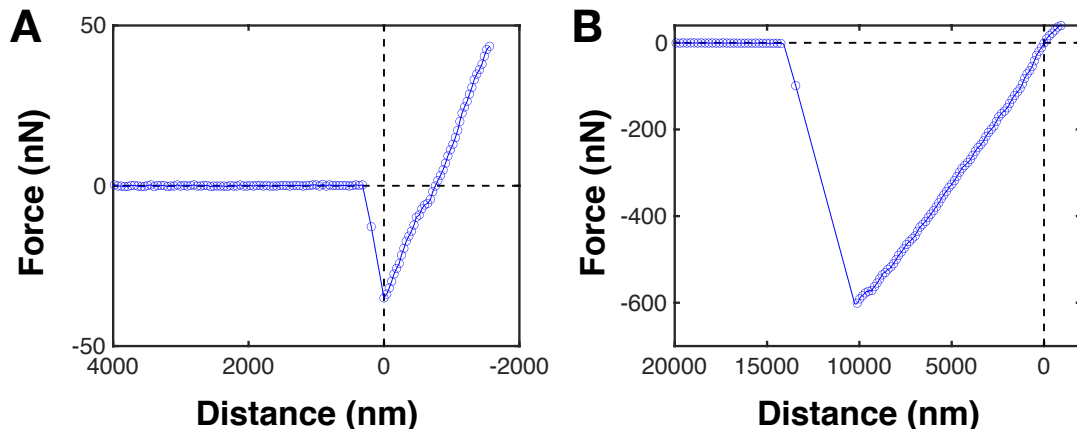
Figure S5: Force distance curves of the bare air-water interface measured with a hydrophilized silica particle as probe from the aqueous phase. (A) Approach force curves, and (B) retract force curves at T = 20 °C. The black vertical dashed lines represent point where the prob is fully is in contact with the monolayer and the slope linear. Black horizontal dashed lines show zero force.

Surface Charge Density of the Hydrophilpos Probe and the Air-Water Interface

The surface potential of the hydrophilpos probe was obtained by measuring force distance curves (force curves) between i) a silicon wafer and a silica probe in water, and ii) a silicon wafer and a hydrophilpos probe in water. As silicon wafers with a 100 nm top layer of silica (Silicon Quest INT.) were as the substrates, the former system is considered to be a symmetrical system. Thus, the surface potential of the silicon wafer can be obtained from force curve analysis (comparison of experimental force curve with theoretically calculated curves). The latter system is a non-symmetrical system. However, the value of the surface potential of the silicon wafer calculated from the former system allows the surface potential of the hydrophilpos probe in water to be determined.

The above two step method was used determine the surface potential of the hydrophilpos probe instead of directly measuring the force curves between a hydrophilpos modified silicon wafer and a hydrophilpos modified silica probe in water. This is because the somewhat high contact angle of the modified hydrophilpos surface ($\theta = 79°$), may cause hydrophobic

induced attractions.

The untreated and modified silica probes were prepared according to the experimental part of the main manuscript. The silica probe was cleaned prior to the experiment where the forces were measured between a silica wafer and a silica probe by rinsing the probe with ethanol and water, and then by plasma treatment in air for 2 min using the medium power of the plasma cleaner.

The force curves were measured between a silica substrate and a silica or hydrophilpos colloid probe in water by using the AFM (Digital Instruments NanoScope III Multimode, Santa Barbara, USA) and a contact mode fluid cell. Briefly, the colloid probe was brought into and out of contact with the substrate, while the change in the deflection of the cantilever (Δx) was measured with a split photodiode as a function of the piezo displacement. Δx was converted from volts to nm by using the slope of the linear compliance region, where the probe and the substrate were in hard wall contact. The force curves were then obtained by subtracting the cantilever deflection from the piezo position (Δx) and by using Hooke's law, $F = k\Delta x$. Here, F and k are the force and the nominal spring constant of the cantilever, respectively. Zero force was defined at large cantilever-substrate separations, where no surface forces acted on the cantilever.

The Derjaguin-Landau-Verwey-Overbeek (DLVO) theory was used to calculate the total interaction free energy per unit area acting between two surfaces (E_{tot}) separated by a distance (D). E_{tot} was calculated via:

$$E_{tot} = E_{DL} + E_{vdW} \,. \tag{1}$$

E_{DL} is the double layer interaction, and E_{vdW} is the van der Waals interaction. E_{DL} was calculated using:

$$E_{DL}(D) = \frac{\epsilon_r \epsilon_0 \kappa}{2} \left[2\Psi_1 \Psi_2 \operatorname{cosech}(\kappa D) \pm \left(\Psi_1^2 + \Psi_2^2 \right) \left(1 - \coth(\kappa D) \right) \right] \,, \tag{2}$$

Here, ϵ_r, ϵ_0, and $1/\kappa$ are the relative permittivity of the electrolyte solution, the permittivity of vacuum, and the Debye length, respectively. Ψ_1 and Ψ_2 are the surface potentials of the silica probe and the silicon wafer, respectively. The constant surface potential boundary condition was calculated using the plus sign in front of the parenthesis in Eq. 3, and the constant surface charge densities boundary condition was calculated using the minus sign. E_{vdW} was calculated assuming non-retardation and using:

$$E_{vdW}(x) = -A/12\pi x^2 \,. \tag{3}$$

The Hamaker constant value (A) of $1.2{\cdot}10^{-20}$ J for a system of two silica surfaces in water was used as the Hamaker constant in this study. The force (F) between the spherical probe and the substrate can be related to E_{tot} using the Derjaguin approximation $(F/R = E_{tot})$, provided the particle radius (R) is much larger than the separation distance between the particle and the substrate. This assumption is fulfilled. The force curve fitting was performed such that the experimental force was centered between the theoretical force curves calculated using the constant charge and the constant potential boundary conditions.

The F/R distance curve measured between two silica surfaces in water is shown in Fig. S6A. Repulsive forces were measured, explained as electrostatic repulsive forces. The E_{tot} distance curves were calculated using Eq. 1-3, which were then compared to the experimental F/R distance curve, in order to determine the absolute value of the surface potential of the silica surfaces $(\left|\Psi_{0,silica}\right|)$ and the Debye length of the system. The $\left|\Psi_{0,silica}\right|$ value of the silica surfaces was determined to be 63 mV. Zeta potential measurements show that silica is negatively charged at pH 5.8. Thus, the surface potential of the silica surfaces is concluded to be -63 mV. The Debye length value was determined to 136 nm, corresponding to a concentration of $5{\cdot}10^{-3}$ mM. This value is close to the calculated concentrations of water with pH 5.8, which is $1.59{\cdot}10^{-3}$ mM, indicating that our fitting was suitable.

The F/R distance curve measured between a silica substrate and the hydrophilpos probe in water is shown in Fig. S6B. A long-ranged attraction was observed, which is explained to
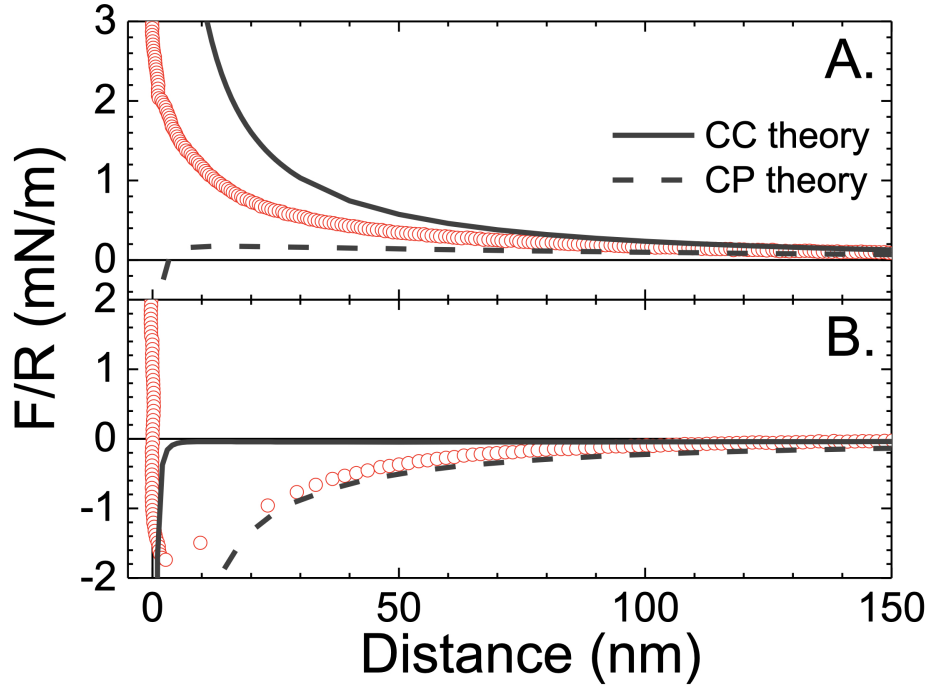
Figure S6: Force curves between the silicon substrate and the silica probe in water (A) and between the silicon substrate and the hydrophilpos probe in water (B). The experimentally measured F/R distance curves are shown as red open circles. The theoretically calculated E_{tot} distance curves are shown as solid and dashed lines, when the constant charge theory (CC) and the constant potential theory (CP) were respectively used.

be electrostatic in origin. Using the surface potential of silica of -63 mV that was obtained above, we estimated the surface potential of the hydrophilpos surface in water to be 50 mV by using Eq. 1-3. The Debye length value was again determined to 136 nm, indicating that our fitting was suitable.

The surface charge density (σ) is related to Ψ_0 via the Grahame Equation

$$\sigma = \sqrt{(8c_e \epsilon_r \epsilon_0 k_B T)} \cdot sinh\left(\frac{e\Psi_0}{2k_B T}\right) . \tag{4}$$

Thus, the surface charge density of the hydrophilpos surface was calculated using the above surface potential and Debye length values of the hydrophilpos surface and Eq. 4 to be $2.98 \cdot 10^{-4}$ C m^{-2}.

Surface charge density of air-pure water interface is 1 electron per 1000 nm^2,[S1] which is

equivalent to $1.06 \cdot 10^{-4}$ C m^{-2}.

Approximated Surface Charge Density of Microgel Monolayers

In order to estimate the surface charge density of the microgel monolayers, we must first estimate the number of charged groups in a microgel. Scotti *et al.* proposed the following equation:[S2]

$$Q = 2 \frac{N_A m_p m_{initiator}}{m M_{initiator}} \tag{5}$$

In our case, the microgels contain also charged groups due to the incorporated APMH. The Eq. 5 can therefore be extended to:

$$Q = \frac{N_A m_p}{m} \cdot \left(2 \cdot \frac{m_{initiator}}{M_{initiator}} + \frac{m_{APMH}}{M_{APMH}} \right) . \tag{6}$$

Where Q is the maximum number of charged moities in a microgel, N_A is the Avogadro constant, m_p, $m_{initiator}$, m_{APMH} and m is the mass of the particle, mass of the initiator, mass of the APMH, and the total mass of all reactants used in the synthesis, respectively. $M_{initiator}$ is the molecular weight of the initiator and M_{APMH} is the molecular weight of the APMH. The value 2 in Eq. 6 is used to account for the fact that the initiator (V50) contains two charged groups. Using Eq. 6, we obtain the maximum number of charged groups within the pNIPAM microgels $Q_{pNIPAM} = 2.0 \cdot 10^5$ and pNIPAM-co-DEAAM microgels $Q_{pNIPAM-co-DEAAM} = 2.6 \cdot 10^5$.

In addition to Q we also need information on the degree of dissociation, its change with temperature, and the distribution of the charged groups in the microgels, in order to estimate the surface charge density. Moreover, microgels in swollen state do not possess a sharp and defined interface. However, we can get a crude estimate of the maximum surface charge

density by assuming: (i) all charged groups of a microgel are located on the surface of a hydrodynamic equivalent sized sphere, and (ii) all groups that can be charged are charged, i.e., full disassociation. With these approximations, the approximated surface charge density of the microgels ($\sigma^*_{microgel}$) would be given by:[S3]

$$\sigma^*_{microgel} = \frac{Q \cdot q_e}{\pi \cdot D_h^2} , \tag{7}$$

where q_e is elementary charge and D_h the hydrodynamic diameter of the microgels (Fig. 2). When the microgels are adsorbed to an interface, a fraction of the charges would be cancelled and/or are not accessible from the aqueous phase. As an estimate, we use $Q_{interface} = Q/2$. The adsorbed microgels presumably have the shape of a spherical cap. Thus, we calculate the surface area of the half cap (A_{cap}) by:

$$A_{cap} = \pi \cdot \left(r^2 + h^2\right) , \tag{8}$$

where r is the cap base radius and h is the cap height, i.e., the thickness. For r, we use $NND_{1st}/2$ from the image analysis (Table 1). h has been previously determined with ellipsometry for the pNIPAM microgels,[S4] where $h_{20° C}$ was $\approx$ 200 nm and $h_{40° C}$ was $\approx$ 110 nm. Due to the similarity of the two microgels, we also use the same values for the pNIPAM-co-DEAAM microgels. Consequently, we calculate the approximated surface charge density of a microgel monolayer (σ^*_{MM}) using:

$$\sigma^*_{MM} = \frac{Q \cdot q_e}{2 \cdot A_{cap}} . \tag{9}$$

We obtain different values for σ^*_{MM} using the results of the image analysis (Table 1) and ellipsometry.[S4] The results are listed in the table below (Table S1).

The values we obtained by our theoretical calculations for the approximated surface charge density of the microgels are large compared to the results of our probe ($2.98 \cdot 10^{-4}$ C m^{-2}) or other silica nanoparticles in the literature.[S5] In fact, considering the crude assump-

Table S1: Center-to-center distance for the first crystalline phase (NND_{1st}) and surface charge density (σ_{MM}) of pNIPAM and pNIPAM-co-DEAAM microgels at different compressions and temperatures.

Microgel	Temperature ($^{\circ}$C)	Π (mN m^{-1})	NND_{1st} (nm)	σ_{MM}^{*} (C m^{-2})
	10	15	(507 ± 28)	0.063
		24	(438 ± 26)	0.075
pNIPAM-co-DEAAM		26	(372 ± 54)	0.089
	40	15	(490 ± 30)	0.092
		24	(431 ± 26)	0.113
		29	(296 ± 26)	0.195
	20	15	(489 ± 30)	0.051
		24	(421 ± 24)	0.060
pNIPAM		26	(380 ± 35)	0.067
	40	15	(481 ± 21)	0.073
		24	(431 ± 23)	0.087
		29	(275 ± 37)	0.164

tions for the calculations, the values should be understood as showing a general trend of the change in surface charge density with a lateral compression and temperature change. To emphasize this, and especially that microgels do not have a defined surface, and therefore use the term approximated surface charge density. The lowest σ_{MM}^{*} was calculated at low temperatures and low surface pressure (10°C and 15 mN m^{-1}) and the highest at 40°C and 29 mN m^{-1}. This result matches our expectation from the electrophoretic mobility measurements in solution (Fig. S2).

References

(S1) Chaplin, M. Theory vs experiment: what is the surface charge of water. *Water* **2009**, *1*, 1–28.

(S2) Scotti, A.; Pelaez-Fernandez, M.; Gasser, U.; Fernandez-Nieves, A. Osmotic pressure of suspensions comprised of charged microgels. *Physical Review E* **2021**, *103*, 012609.

(S3) Pelton, R.; Pelton, H.; Morphesis, A.; Rowell, R. Particle sizes and electrophoretic mobilities of poly (N-isopropylacrylamide) latex. *Langmuir* **1989**, *5*, 816–818.

(S4) Bochenek, S.; Scotti, A.; Ogieglo, W.; Fernndez-Rodrguez, M. A.; Schulte, M. F.; Gumerov, R. A.; Bushuev, N. V.; Potemkin, I. I.; Wessling, M.; Isa, L.; Richtering, W. Effect of the 3D Swelling of Microgels on Their 2D Phase Behavior at the LiquidLiquid Interface. *Langmuir* **2019**, *35*, 16780–16792.

(S5) Shi, Y.-R.; Ye, M.-P.; Du, L.-C.; Weng, Y.-X. Experimental determination of particle size-dependent surface charge density for silica nanospheres. *The Journal of Physical Chemistry C* **2018**, *122*, 23764–23771.